A COMPACT MULTILAYER CONFIGURATION FILTER WITH INNER MIXED ELECTRIC AND MAGNETIC COUPLING

Wei Tang, Jun He[*], and Xiaobo Yang

Research Institute of Electronic Science and Technology, University of Electronic Science and Technology of China, Chengdu 611731, China

Abstract—A novel cascade microstrip filter with mixed electric and magnetic coupling is proposed and examined. For the first time, we designed a novel multilayer configuration resonator with a compact size. Compared with conventional open-loop filter, the size decreased 75%. First, using novel multilayer configuration resonator instead of monolayer configuration resonator, the size is decreased about 45%. Meanwhile, two microstrip patches serve as inner coupling capacitor, which create and strengthen electric field. Owing to this inner coupling, the size of filter can be further reduced. Moreover, with a section of high characteristic impedance transmission line connected to the ground though a via-hole, it can serve as coupling inductor and create main magnetic field. Based on this structure, mixed EM coupling is realized and can generate additional transmission zero, which means that adopting low-order filter can achieve the same characteristic as high-order filter. Based on the above solutions, the filter size can be sharply decreased to 12.5 mm × 7.7 mm (i.e., $0.05\lambda_g \times 0.033\lambda_g$). Furthermore, advantages of using this type filter are not only low insert loss, but also increased attenuation out-of-band with controllable transmission zeros.

1. INTRODUCTION

Advanced modern wireless microwave communication systems have strigent requirements for filters, such as compact size, sharp rejection out-of-band, low insertion loss. From conventional filter design theory, transmission zeros that exist in out-of-band can improve filter ability greatly. Recently, by using crossing electric and magnetic (EM)

coupling or source-load coupling to design generalized quasi-elliptic filter can get more transmission zeros [1, 2], in this type of filter, Stepped-Impedance resonators (SIRs) take main part. e.g., [1], using $\lambda/4$ SIRs, generating transmission zeros very close to passband. However, the size of this filter is a little large. At the same time, because adjusting the position of the transmission zeros can get high frequency selectivity, numerous papers ([2–5]) have been devoted to realizing controllable transmission zeros. Compared with the conventional half-and quarter-wavelength stepped-impedance resonators (SIRs), [2] proposed that unequal-length shunted-line stepped-impedance resonator (shunted-line SIR) can provide an efficient way to generate multitransmission zeros and one controllable transmission zero near the passbands to improve the out-of-band rejection. In [4], Wei et al. designed a novel trigonal dual-mode filter with controllable transmission zeros, and both dual-mode response and controllable transmission zeros are realized by using cross-coupling. But it is complicated to control the zeros distribution, especially in first time design this type filter, and the roll-off in the low stopband (without transmission zeros) needs to be improved. Chu and Wang utilized open-loop filter with controllable electric and magnetic coupling [5]. In their work, one or more transmission zeros is achieved. The open gaps have the maximum electric field, and the sides of coupled resonators have the maximum magnetic field. However, they can get only one zero in lower or upper stopband when cascading two resonators. This will lead to worse frequency selectivity in stopband without transmission zero. Using more resonators can obtain more transmission zeros and realize good frequency selectivity, but the size will increase 50%. In their other works, they fabricated an inline coaxial quasi-elliptic filter with separately controllable mixed electric and magnetic coupling. As proposed in [6], an N-order filter can realize N-1 finite transmission zeros at maximum. However, in order to achieve desired performance, this design must insert additional coupling components and does much modification work. Same as [5], their fractional bandwidths are only 3.8%, 4.1%, respectively. In [5–7], compared with a purely coupled filter when transmission zeros were close-to-band, a mixed coupled filter achieved narrower bandwidth, generally not more than 5%. [8] analyzed the reason of this drawback in details and designed an novel triangular open-loop filter with backed aperture to overcome the shortcoming of EM coupled filters.

Certainly, except for EM coupling, many ways can reduce the size of filter, e.g., in [9], using DGS folded slot resonators loaded by lumped capacitors, the filter is 55% smaller than the conventional filer. However, without *EM* coupling, no transmission zeros are available,

which leads to roll-off capability hardly suitable for applications.

This paper presents a generalized quasi-elliptic filter based on novel multilayer configuration resonator. Fig. 1(a) is the three-dimensional geometry of the proposed resonator. In this resonator, we adopt via-hole connecting ground to realize magnetic coupling and use microstrip patches in the bottom and middle of dielectric substrate to obtain major electric coupling. Additional coupling zero point or transmission zero is generated as a result of the cancelling effect of inner magnetic coupling and electric coupling. Moreover, turning the only physical coupling parameter to regulate the magnetic coupling can control the position of the zero point. Certainly, compared with conventional SIRs or Open-Loop resonator, adopting multilayer configuration resonator can sharply decrease the size of filter. All of these works contributed to this filter to make it not only more compact but also high frequency selectivity with an easy way to control the transmission zeros distribution.
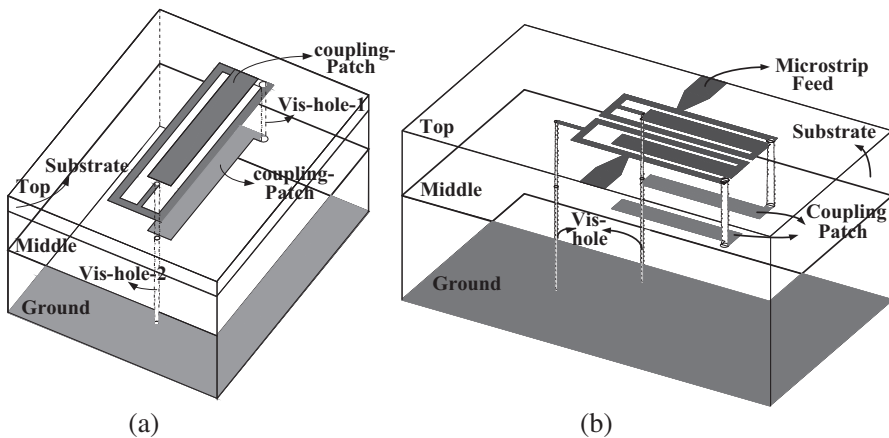

Figure 1. (a) Three-dimensional geometry of proposed multilayer configuration resonator structure. (b) Three-dimensional geometry of the proposed fourth-order filter using multilayer configuration resonator. The coupling patches in the top and middle layer of dielectric, respectively. Via-hole-1 connecting two coupling patch, via-hole-2 connecting YI to the ground.

2. THEORY OF FILTER DESIGN

The top and bottom plane-layouts of the proposed resonator viewed from the top side are also depicted in Fig. 2. The newly proposed resonator is mainly composed of three elements, i.e., two microstrip patches on the top and middle of dielectric substrate, respectively, a
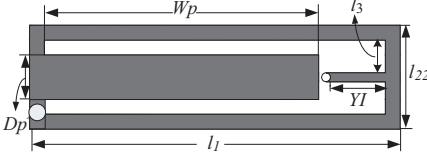
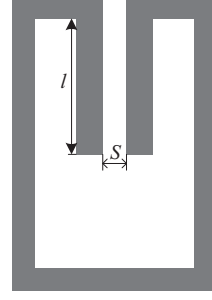**Figure 2.** Proposed multilayer resonator (top-view).

Figure 3. Conventional open-loop resonator.
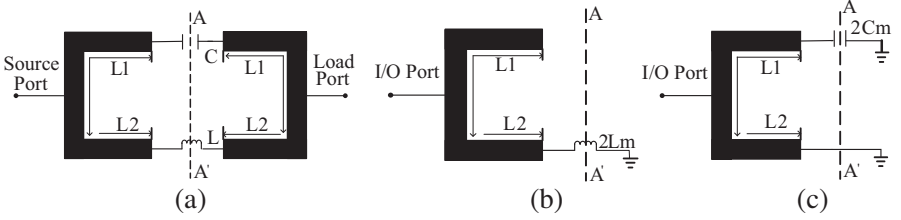

Figure 4. (a) Second-order filter equivalent even and odd-mode configurations. (b) Even mode. (c) Odd mode.

via-hole through the substrate, and a high characteristic impedance line connecting via-hole. The microstrip patch has rectangular shape with area $W_P \times D_P$. The via-hole is drilled by a 0.15-mm-diameter bit and filled with conductive liquid silver to provide good performance. Fig. 3 shows a general open-loop resonator. The parallel lines provide the main electric coupling [10]. Both the length and width of the parallel lines have a great effect on the operating frequency and bandwidth of the filter [11]. Overlapping the two parallel lines can obtain same properties as well as decrease the size by 1/2. At the same time, regulating only the length of the high characteristic impedance line can change the ratio of electric coupling and magnetic coupling, which will control the distribution of transmission zeros.

Fig. 4 shows a second-order filter configuration and topology. An odd and even-mode analysis [12] is adopted to analyze this structure. From the mechanism of the resonator resonance, the structure is resonant when its source and load input admittance is zero for both even and odd modes, i.e.,

$$Y_{even} = Y_{odd} = 0 \tag{1}$$

In Fig. 4(b) is the even-mode case, the magnetic wall is applied at AA' plane, analysis equivalent-circuit of the resonator the even-mode

input admittance is derived as [12]

$$Y_{even} = jY_c \left[\tan \beta_e l_1 + \frac{2\omega_e L_m Y_c \tan \beta_e l_2 - 1}{2Y_c \omega_e L_m + \tan \beta_e l_2} \right] \qquad (2)$$

β_e denotes the propagation constant at the even-mode resonator angular frequency ω_e and $Y_C = 1/Z_C$ the characteristic impedance of the resonator.

Making use of (1) and (2) can achieve

$$\frac{2L_m \omega_e}{Z_c} = \frac{1}{\tan \beta_e (l_1 + l_2)} \qquad (3)$$

Using Taylor expansion at $l_1 + l_2 \approx \lambda_g/16$, for a large L_m, and only retaining low-order terms, (3) can be written by

$$\frac{2L_m \omega_e}{Z_c} + \beta_e (l_1 + l_2) = \frac{\pi}{8} \qquad (4)$$

Since $\beta_e = \frac{\omega_e \sqrt{\varepsilon_{re}}}{c}$, where c is the speed of the light in the free space. The even-mode resonant angular frequency can be given by

$$\omega_e = \frac{\pi}{8(2L_m Y_c + \gamma)} \qquad (5)$$

As

$$\gamma = \frac{\sqrt{\varepsilon_{re}}(l_1 + l_2)}{c}$$

For the odd-mode case, the equivalent-circuit representation of the resonator, when the electric wall is applied at the AA' plane, is illustrated in Fig. 4(c). The odd-mode input admittance is

$$Y_{odd} = jY_c \left[\frac{2\omega_o C_m + Y_c \tan \beta_o l_1}{Y_c - 2\omega_o C_m \tan \beta_o l_1} - \cot \beta_o l_2 \right] \qquad (6)$$

Using (1) and (6) can achieve

$$\frac{2C_m \omega_o}{Y_c} = \frac{1}{\tan \beta_o (l_1 + l_2)} \qquad (7)$$

For a large C_m, $l_1 + l_2 \approx \lambda_g/16$, the right side of (7) can be expanded by using Taylor expansion at $l_1 + l_2 \approx \lambda_g/16$. Omitting the high-order terms, (7) can be written as

$$\frac{2C_m \omega_o}{Y_c} + \beta_o (l_1 + l_2) = \frac{\pi}{8} \qquad (8)$$

Since $\beta_o = \frac{\omega_0 \sqrt{\varepsilon_{re}}}{c}$, the odd-mode resonant angular frequency can be determined by

$$\omega_O = \frac{\pi}{8(2C_m Z_C + \gamma)} \qquad (9)$$

The γ as same as (5), the center frequency of bandpass can be approximated as

$$f_0 = \frac{1}{4\pi}(\omega_e + \omega_o) = \frac{1}{32}\left[\frac{1}{2C_m Z_c + \gamma} + \frac{1}{2L_m Y_c + \gamma}\right] \qquad (10)$$

The coupling coefficient K can be computed from the knowledge of even and odd-mode frequencies as

$$K = \frac{\omega_o^2 - \omega_e^2}{\omega_o^2 + \omega_e^2} = C(Y_c L_m - C_m Z_c) = M - E \qquad (11)$$

As $C = \frac{4(Y_c L_m + Z_c C_m + \gamma)}{(2Z_c C_m + \gamma)^2 + (2Y_c L_m + \gamma)^2}$, and $M = CY_c L_m$, $E = CZ_c C_m$.

From (11), the inter-stage coupling of filter can be formed by two separate parts, and electric (E) coupling and magnetic (M) coupling are independent [12] as illustrated in the filter topology of Fig. 5. However, there is canceling effects for the total coupling coefficient K, which will be helpful for a narrow bandwidth filter, where a smaller coupling coefficient is required [13].
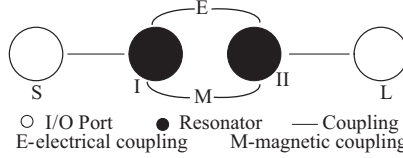

Figure 5. Second-order filter topology.

As in [10], second- and fourth-order filters were designed. In second-order design, both the length of coupling lines l_J and the length and width of high characteristic impendence transmission line l_h and w_h have a great effect on the filter capability. In fourth-order filter design, besides above discussion, the distance between resonators would affect the filter capability. However, in the following realization, if the operating frequency is fixed, the length and width of coupling plane would not be changed. Fig. 6 shows the spectrum response of different sizes of coupling planes under the condition of $l_1 + l_2 \approx \lambda g/16$ (corresponding to (4) and (8)).

As shown in Fig. 6, W_p is adopted to resonance frequency 900 MHz. W_p is fixed which means the main electric coupling (E) confirmed. From (11), we can know that the coupling coefficient K is determined only by magnetic coupling (M). Therefore, designing the filter just means adjusting the L_m when the resonator is fixed, which would be greatly simplify filter design process.

The magnetic coupling (M) is generated by a section of high characteristic impedance transmission line (length of YII and width
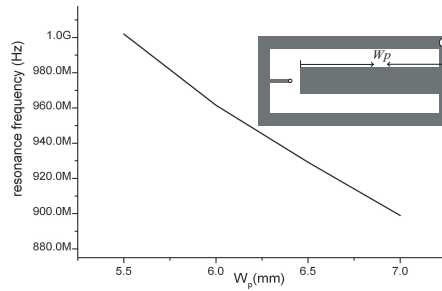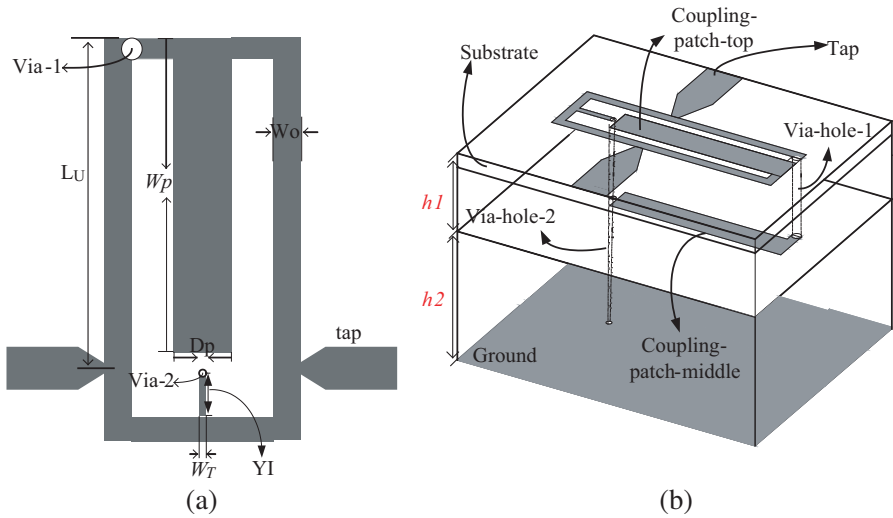
Figure 6. Resonance frequency of different W_p.

(a)   (b)

Figure 7. Configuration of second-order filter. (a) Top-View, (b) 3-D View. $W_p = 9.75\,\text{mm}$, $L_U = 8\,\text{mm}$, $R_{via\text{-}1} = 0.25\,\text{mm}$, $R_{via\text{-}2} = 0.15\,\text{mm}$, $Wo = 0.5\,\text{mm}$, $D_p = 1.5\,\text{mm}$, $W_T = 0.3\,\text{mm}$, $h_1 = 0.127\,\text{mm}$ (top to middle layer), $h_2 = 0.508\,\text{mm}$ (middle to ground layer).

of W_T) connected to the ground through a via-hole. In [14], it is proved that the decrease in W_L increases the inductor L_m and vice versa. Therefore, in filter fabrication attention should be concentrated on the effect of length (YII).

3. FOURTH-ORDER FILTER REALIZATION

In Fig. 7, the second-order filter with a tap of feeder is illustrated. Properly choosing the length of W_p can achieve the main part of the resonator, restricted by the fabrication craft, and the width of coupling plane (W_T) cannot be under $0.1\,\text{mm}$. At the same time, considering

the consistence and manufacturing errors, the width fixed to 0.3 mm, which not only satisfy the maximum magnetic coupling but also match the via-hole diameter.

Commercial electromagnetic (EM) software HFSS 13.0 is used in the following analysis and design. Based on the theory of Section 2, through second-order filter design process, we will discuss the effect of YI. Fig. 8 compares different lengths of YI, though the length of YI has been changed four times and the resonance frequency hardly changed. But the different lengths of YI have a great effect on transmission zeros distribution, and as YI extending, the zeros are closer to the passband. At the same time, the value of S_{21} gets larger which means the external quality factor get greater. In a similar way, by adjusting the length of W_p, the spectrum response shown in Fig. 9, as the W_p gets shorter, the transmission zero gets close to the operating frequency, while the operating frequency shifts up. Due to formula (11), the canceling effect of M and E will create a zero coupling point or transmission zero f_Z in the stopband.

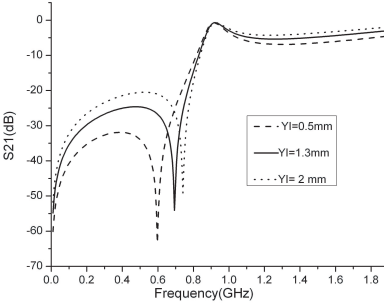$$f_Z = f_0 \sqrt{\frac{E}{M}} \qquad (12)$$

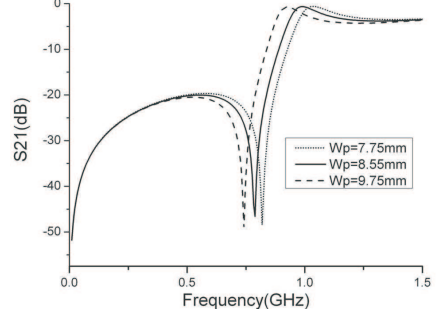**Figure 8.** Spectrum response of vary YI ($Wp = 9.75$ mm).

Figure 9. Spectrum response of vary Wp ($YI = 2$ mm).

f_0 denotes the resonant frequency of the mixed coupled resonator. From above analysis, in second-order filter, extending YI will strengthen the magnetic coupling, while diminishing W_p will weaken the electric coupling. All of these solutions make zeros location closer to operating frequency, which is expected as in formula (12). Therefore, to get better frequency selectivity capability, ratio E/M should be close to unity. But when this ratio is close to unity, the total coupling K must be a small value due to the restriction of formula (11), and this may lead to a narrower passband. The effective way to solve this conflict is to enhance electric and magnetic coupling until both

E and M are very large [15]. Based on this theory, the configuration and topology of a fourth-order filter are shown in Figs. 10(a) and (b), respectively.

The total coupling coefficient K is the result of coupling after E and M canceling [refer to (15)]. Fig. 11 denotes the coupling coefficients of varied distances between adjacent resonators (W_H). When distance is very short, the frequency response would have two resonant peaks of wave, and when distance is longer, the insert loss will be worse. From HFSS simulation, the coupling patch generates the main electric coupling, while for the two coupled resonators, the coupled sides have with the maximum magnetic coupling. Considering return loss and insertion loss, we choose $W_H = 0.5$ mm. Adjusting the length of YII will change the ratio of EM coupling. Fig. 12 shows the frequency response of varied YII. When YII is short, the electric field dominates the coupling, and there is only one transmission zero in the upper band. With the increase of YII, the magnetic coupling cancels electric coupling and generates zero point in the lower stopband. As compared to a traditional combine filter, one more zero point generated in the lower stopband is mainly due to the inter-stage coupling between the E and M dominant pairs. When continuously increasing the length of YII, the ratio of EM coupling is close to unity, and the transmission
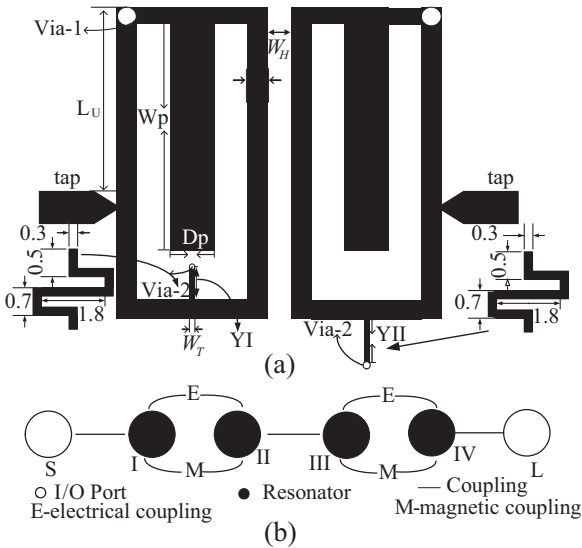

Figure 10. Configuration and topology of the fourth-order filter. (a) Configuration. (b) Topology.
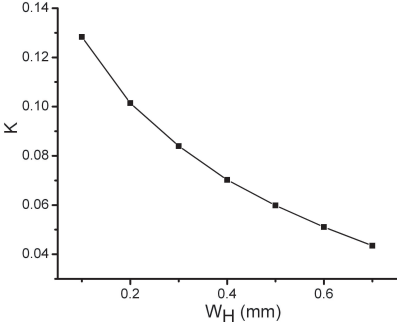
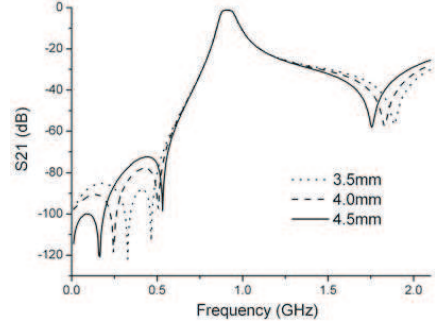**Figure 11.** Total coupling co-efficients for adjacent resonators space (W_H).

Figure 12. Frequency response of vary *YII*. With *YII* increased, transmission zeros close to centre frequency.

zeros get close to centre frequency. So by adjusting only one physics parameter, the transmission zero distribution can be controllable.

However, to obtain enough magnetic coupling, the length of high characteristic impedance transmission line (*YII*) would be at least 3.5 mm. So we adopted zigzag line instead in practical realization. Because of the line coupling, the electric coupling cancels out a part of magnetic coupling. The length of zigzag line must be a little longer than the straight line, but the size is decreased. To simplify the manufacture procedure and improve product accuracy, the top and middle layers of the filter produced in a same dielectric substrate (Rogers 5880, $\varepsilon_r = 2.2$) with thickness 0.127 mm, thickness of bottom layer is 0.508 mm, $W_p = 9.75$ mm, $L_U = 8$ mm, $R_{via\text{-}1} = 0.25$ mm, $R_{via\text{-}2} = 0.15$ mm, $Wo = 0.5$ mm, $D_p = 1.5$ mm, $W_T = 0.3$ mm, $W_H = 0.5$ mm, $YI = 2$ mm, $YII = 2.2$ mm (straight line 4.2 mm). As compared with traditional doubling plate filter, this type of filer does not increase manufacture complexity, but sharply decreases the filter size.

The results of simulation and measurement of fourth-order filter in Fig. 10 are compared and shown in Fig. 13. The frequency ranges from 0.1 GHz to 1.8 GHz, and preliminarily designed at a center frequency of 0.9 GHz with 10% 3-dB fractional bandwidth. The transmission zeros are in 0.37 GHz (with rejection -98 dB), 0.58 GHz (with rejection -96 dB) and 1.54 GHz (with rejection -54 dB), respectively with insert loss under 0.96 dB. Using Agilent E8363B, the discrepancies between simulation and measurement may come from the difference between simulated and realized structures. As described at the last paragraph,

two dielectric substrates are used in fabrication instead of ensemble dielectric substrate in simulation. So the frequency response shifts to lower frequency range. At the same time, the zero points in lower stopband are buried in the noise floor in measurement. The measured results are as follows. The minimum insertion loss is 1.45 dB, center frequency at 0.86 GHz, transmission zero (upper stopband) at 1.45 GHz, with rejection −50 dB. Table 1 compares the sizes of several similar filters and other capabilities.
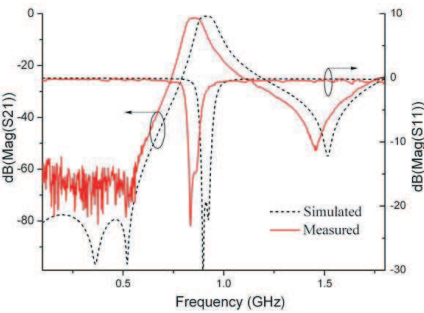

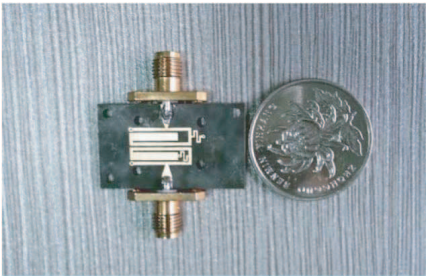**Figure 13.** Simulated and measured results of the fourth-order filter.

Figure 14. Fabricated fourth-order multilayer filter.

Table 1. Comparison of similar filters.

Ref.	FBW	Order/Amount of ZPs	Insertion loss	Circuit size
[1]	5.6%	5/3	2.01 dB	$0.094\lambda_0 \times 0.1176\lambda_0$
[5]	5%	4/2	3.4 dB	$0.13\lambda_0 \times 0.29\lambda_0$
[10]	17%	4/2	1.4 dB	$0.06\lambda_0 \times 0.0545\lambda_0$
[16] Second	12%	4/2	2.7 dB	$0.12\lambda_0 \times 0.1182\lambda_0$
[17] Filter II	14.3%	3/1	1.28 dB	$0.093\lambda_0 \times 0.067\lambda_0$
This work	**10%**	**4/3**	**1.45 dB**	$\mathbf{0.037\lambda_0 \times 0.023\lambda_0}$

From Table 1, it can be seen that this type of filter has similar capabilities to others such as FBW, with low insertion loss. However, the rejection of this work in low stopband is more sharp than others because of additional zero points. Moreover, as shown in Fig. 14, the

size of the fabricated fourth-order multilayer filter occupies an area as small as $0.037\lambda_0 \times 0.023\lambda_0$, which is only 1/4 of that of fabricated separate electric and magnetic coupling paths (SEMCP) filters [10] (as $0.06\lambda_0 \times 0.0545\lambda_0$), only 1/16 of that fabricated open-loop filter (as $0.13\lambda_0 \times 0.29\lambda_0$).

4. CONCLUSION

This paper presents a novel multiplayer configuration filter and adopts inner electric and magnetic couplings. The filter size is sharply decreased. Compared with conventional inline filter, additional transmission zero is generated in low stopband without source-load coupling, and makes the rolloff of this filter in low stopband much steeper. At the same time, the distribution of transmission zeros can be controlled by only one physical parameter, which will make designing different types of mixed EM coupling filters easy to fulfill distinct applications.

REFERENCES

1. Xiao, O. Y., "Compact quasi-elliptic filter using mixed EM coupling $\lambda/4$ stepped-impedance resonators," *2012 International Conference on Microwave and Millimeter Wave Technology (ICMMT)*, Vol. 4, 1–4, May 5–8, 2012.

2. Hsu, C.-Y., C.-Y. Chen, and H.-R. Chuang, "Microstrip dual-band bandpass filter design with closely specified passbands," *IEEE Trans. on Microw. Theory and Tech.*, Vol. 61, No. 1, Jan. 2013.

3. Zhang, L., Z.-Y. Yu, and S.-G. Mo, "Novel microstrip bandpass filter with controllable transmission zeros," *2009 3rd IEEE International Symposium on Microwave, Antenna, Propagation and EMC Technologies for Wireless Communications*, 1016–1018, Oct. 27–29, 2009

4. Wei C.-L., B.-F. Jia, Z.-J. Zhu, and M.-C. Tang, "Novel trigonal dual-mode filter with controllable transmission zeros," *IET Microw, Antennas Propag.*, Vol. 5, No. 13, 1563–1567, May 2010.

5. Chu, Q.-X. and H. Wang, "A compact open-loop filter with mixed electric and magnetic coupling," *IEEE Trans. on Microw. Theory and Tech.*, Vol. 56, No. 2, Feb. 2008.

6. Wang, H. and Q.-X. Chu, "An inline coaxial quasi-elliptic filter with controllable mixed electric and magnetic coupling," *IEEE Trans. on Microw. Theory and Tech.*, Vol. 57, No. 3, Mar. 2009.

7. Wang, H. and Q.-X. Chu, "An EM-coupled triangular open-loop filter with transmission zeros very close to passband," *IEEE Microw. and Wireless Components Letters*, Vol. 19, No. 2, Feb. 2009.

8. Chu, Q-X. and H. Wang, "Planar quasi-elliptic filters with inline em coupled open-loop resonators," *2008 IEEE MTT-S International Microwave Workshop Series on Art of Miniaturizing RF and Microwave Passive Components (Invited Paper)*, 47–50, Chengdu, China, Dec. 2008.

9. Abdel-Rahman, A. B. and A. S. Omar, "Miniaturized bandpass filters using capacitor loaded folded slot coupled resonators," *2010-IEEE APS, Middle East Conference on Antennas and Propagation (MECAP)*, 1–4, Cairo, Egypt, Oct. 2010.

10. Ma, K., J.-G. Ma, K. S. Yeo, and M. A. Do, "A compact size coupling controllable filter with separate electric and magnetic coupling paths," *IEEE Trans. on Microw. Theory and Tech.*, Vol. 54, No. 3, 1113–1119, Mar. 2006.

11. Tsai, C.-M., S.-Y.Lee, and C.-C Tsai, "Performance of a planar filter using a 0° feed structure," *IEEE Trans. on Microw. Theory and Tech.*, Vol. 50, No. 10, 2362–2367, Oct. 2002.

12. Hunter, I. C., *Theory and Design of Microwave Filters*, London, UK, IEE Press, 2001.

13. Kuo, J.-T., C.-L. Hsu, and E. Shih, "Compact planar quasi-elliptic function filter with inline stepped-impedance resonators," *IEEE Trans. on Microw. Theory and Tech.*, Vol. 55, No. 8, 1747–1755, Aug. 2007.

14. Goldfarb, M. E. and R. A. Pucel, "Modeling via hole grounds in microstrip," *IEEE Microw. Guided Wave Lett.*, Vol. 1, No. 6, 135–137, Jun. 1991.

15. Hedayati, M., M. J. Kazemi, and R. Safian, "Design and implementation of a multi triangular microstrip resonator passband filter based on mixed coupling," *2011 IEEE International RF and Microwave Conference (RFM 2011)*, 1–4, Serernban, Malaysia, Dec. 12–14, 2011

16. Kuo, J.-T., S.-C. Tang, and S.-H. Lin, "Quasi-elliptic function bandpass filter with upper stopband extension and high rejection level using cross-coupled stepped-impedance resonators," *Progress In Electromagnetics Research*, Vol. 114, 395–405, 2011.

17. Kuo, J.-T., T.-W. Lin, and S.-J. Chung, "New compact triple-mode resonator filter with embedded inductive and capacitive cross coupling," *Progress In Electromagnetics Research*, Vol. 135, 435–449, 2013.